Chemical Changes of Raw Materials and Manufactured Binderless Boards during Hot Pressing: Lignin Isolation and Characterization

Yong-Chang Sun,[a,#] Zhi Lin,[b,#] Wan-Xi Peng,[b,*] Tong-Qi Yuan,[a] Feng Xu,[a] Yi-Qiang Wu,[b] Jing Yang,[c] Yang-Sheng Wang,[d] and Run-Cang Sun [a,*]

Thermomechanical pulp (TMP) is used for fiber production in binderless boards industries. Milled wood lignin (MWL) and enzymatic mild acidolysis lignin (EMAL) isolated from raw material and from binderless boards (BB) were comparatively analyzed to investigate the effects of chemical changes on the bonding performance in BB. The results showed that acid-insoluble lignin of the BB were increased during the sodium silicate solution pretreatment after hot-pressing. The lignin fractions obtained were characterized by gel permeation chromatography (GPC), Fourier transform infrared (FT-IR) spectroscopy, and ^{1}H-^{13}C correlation heteronuclear single-quantum coherence (HSQC) nuclear magnetic resonance (NMR) spectroscopy. Results showed that 31.1% of EMAL (based on Klason lignin) with low molecular weight (M_w=1630 g/mol) was isolated from the BB. The increased total phenolic OH groups (3.97 mmol/g) of EMAL from sodium silicate solution pretreated BB indicated that there was degradation of lignin and cleavage of lignin-carbohydrate linkages during hot-pressing. In addition, the content of β-O-4' aryl ether linkages of EMAL from the BB increased to 69.2%, which was higher than that of the untreated sample (60.1%). It was found that S units (syringyl-like lignin structures) were preferentially condensed by hot pressing over G (guaiacyl-like lignin structures) units, and the S/G ratio increased after the hot-pressing process.

Keywords: Chemical change; Binderless board; Thermomechanical pulp; MWL; EMAL

*Contact information: a: Beijing Key Laboratory of Lignocellulosic Chemistry, Beijing Forestry University, Beijing 100083, China; b: College of Materials Science and Engineering, Central South University of Forestry and Technology, Changsha 410004, China; c: Chengdu Xinhongying Furniture Co. Ltd., Chengdu 610200, China; d: Linyi Zhensheng Wood Industry Co. Ltd., Linyi 273400, China; #: Yong-Chang Sun and Zhi Lin are co-first authors; *Corresponding author: rcsun3@bjfu.edu.cn (R.-C. Sun)*

INTRODUCTION

Currently, the worldwide demand of binderless boards (BB) has been growing due to the fact that this product does not emit formaldehyde (Rokiah *et al*. 2009). Binderless boards are wood-based composites of varying shapes and sizes consisting of particles of lignocellulosic material bonded together without resin under heat and pressure. Because no resin is used in binderless boards, the self-bonding strength is improved only by activating the chemical components of the lignocellulosics during the heat treatment. However, with the increasing market demand of BB, there is a need to find out the self-bonding mechanism of BB, especially the chemical changes of the components during manufacturing. This is considered to be important for designing better manufacturing conditions to improve the performances of BB.

Binderless boards are usually prepared from raw materials rich in hemicelluloses, since the degradation of hemicelluloses during heat/steam to produce furan is believed to play an important role in self-bonding. It has been reported that the main self-bonding strength of BB is due to the lignin-furfural linkages generated during the hot pressing (Mobarak *et al*. 1982; Suzuki *et al*. 1998). Different methods are being used to prepare the raw material for BB production. Steam explosion has been used not only for fuel production but for improving wood composite properties (Pelaez-Samaniego *et al*. 2013). In the manufacture of BB, there are three generalized processes that may be employed: the hot-pressing system (Mobarak *et al*. 1982; Ellis and Paszner 1994; Okamoto *et al*. 1994), the steam explosion process before hot pressing (Suzuki *et al*. 1998; Laemsak and Okuma 2000), and steam injection pressing (Okamoto *et al*. 1994; Xu *et al*. 2003). It has been found that the cleavage of ester bonds and β-O-4' inter-unit linkages of lignin during steam explosion contributes to self-bonding of the lignocellulosic materials. Steam treatment has proved to be an effective method for improving the dimensional stability of wood-based composites. According to Xu *et al*. (2003), the internal bonding (IB) strength of BB was excellent at low steam pressure. In addition, the oxidation of the surface lignin of the particles was performed based on laccase or peroxidase enzymes. It was found that the enzymes produced by white-rot fungi can degrade cellulose, and are usually able to degrade lignin or lignin-related compounds when they are cultured on the substrate (Enoki *et al*. 1988). However, there has been little research to date on the chemical changes of the components of BB, especially for lignin in chemical-pretreated BB.

The aim of this study was to investigate the chemical changes of lignin in BB during the self-bonding process by hot pressing. Sodium silicate solution (water glass), a cheap and common industrial product, has been used as the precursor to prepare silica sol, molds, superhydrophobic textiles, resins, and aerogels (Satoh 1999; Yachi *et al*. 2005; Bhagat *et al*. 2007). Herein, we use different concentrations of sodium silicate solution to pretreat thermomechanical pulp in order to enhance the IB strength of BB, and to investigate the structure of the lignin fractions from thermomechanical pulp and BB. Milled wood lignin (MWL) and enzymatic mild acidolysis lignin (EMAL) isolated from raw material, thermomechanical pulp, and binderless boards were characterized in terms of molecular weight and Fourier transform infrared (FT-IR) spectroscopy. A large amount of lignin structural information, such as S/G ratios and the amounts of major substructures (β-O-4', β-β', β-5', etc.) were semi-quantitatively analyzed by two-dimensional heteronuclear single-quantum coherence (2D HSQC) nuclear magnetic resonance (NMR) spectroscopy. In addition, quantitative ^{31}P NMR analysis was performed to illuminate the relationship between the functional groups of lignin and the IB strength of BB.

EXPERIMENTAL

Materials

Eucalyptus urophylla, 6 years old, was kindly provided by Guangxi Forestry Administration, Guangxi, China. After removing the leaves and bark, the trunks were chipped into small pieces. Thermomechanical pulp was obtained by a thermomechanical vapor process. The wood chips were first scrubbed with water and fed with a plug screw to a pressurized preheater at a suitable temperature. After that, the chips are further treated at 175 °C at a corresponding vapor pressure and milled for 2 min.

Sample Preparation

The thermomechanical pulp fiber was fully soaked in sodium silicate solution at concentrations of 0.3%, 0.7%, 0.9%, and 1.5% for 6 h, and then filtered to obtain the pretreated thermomechanical pulp to manufacture the binderless boards. The sodium silicate solution pretreated samples before hot pressing were labeled as BB3b, BB5b, BB7b, BB9b, and BB15b. The pretreated pulp fiber was dried in an oven at 105 °C for 10 h and stored in a vacuum desiccator for further analysis. The board manufacturing conditions were as follows: pressing temperature 160 °C, pressing pressure 15 MPa, pressing time 20 min, board thickness 5 mm, and board size 50 mm × 50 mm. The pretreated samples were hot pressed, and the corresponding binderless boards were named as BB3a, BB5a, BB7a, BB9a, and BB15a, respectively. The internal bond (IB) strength was tested according to Chinese Standard GB/T 11718-2009, with the specimen thickness 5 mm and specimen size 50 mm × 50 mm. The moisture content of the specimens ranged from 6 to 8%. The constant testing speed was 1.5 mm/min. To evaluate the physical properties of the BB, the internal bond (IB) strength was compared with the Chinese Standard GB/T 11718-2009.

Isolation of MWL and EMAL

The MWL from the raw material and thermomechanical pulp was isolated according to the procedure proposed by Björkman (1956) as shown in Fig. 1. The ball-milled EU powder/thermomechanical pulp was stirred in 96% dioxane solution with a solid-to-liquid ratio of 1:20 (g/mL) at room temperature in the dark for 48 h. Then, the mixture was filtered and washed with the same solvent until the filtrate was clear. The combined filtrates were first concentrated at reduced pressure and then precipitated in 3 volumes of deionized water. The obtained MWL preparation was purified as described elsewhere (Björkman 1956; Ikeda *et al*. 2002).

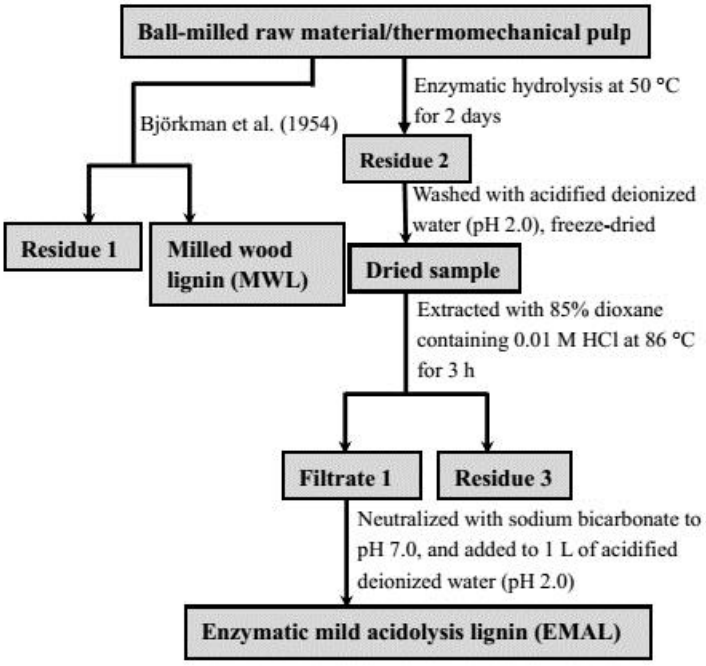

Fig. 1. Isolation procedure for MWL and EMAL

To isolate EMAL fractions, the thermomechanical pulp fiber, pretreated thermo-mechanical pulp fiber, and the binderless boards were ball milled. The samples were ball milled in a planetary mill for 5 h (Fritsch GMBH, Idar-Oberstein, Germany) at room temperature with a rotation speed of 450 rpm. The procedure involved the repetition of 10 min milling and 10 min cooling cycles. EMALs were isolated from the ball-milled samples according to the procedure described by Wu and Argyropoulos (2003) (Fig. 1).

The ground samples were hydrolyzed with cellulase (Novozyme, China; filter paper activity, 50 FPU/mL) and Novozyme 188 (Novozyme, China; filter paper activity, 240 FPU/mL) at a ratio of 50 FPU/g wood. Enzymatic hydrolyses were carried out at 50 °C for 48 h using 50 mM citrate buffer (pH 4.5) at 2% consistency in an orbital water bath shaker.

The insoluble material remaining after the enzymatic hydrolysis was collected by centrifugation, washed with hot acidified deionized water (pH 2.0, 80 °C), and freeze-dried. The crude lignin obtained was further submitted to a mild acid hydrolysis with 85% dioxane solution containing 0.01 M HCl at 86 °C for 3 h. The filtrate was collected by centrifuging the resulting suspension, neutralized with sodium bicarbonate, and finally added drop wise to 1 L of acidified deionized water (pH 2.0). The precipitated lignin pellet was obtained by filtration, washed two times with deionized, and freeze-dried for analysis.

Characterization of Lignin

Yield and associated polysaccharides analysis

Determination of the chemical composition of the raw material and pretreated samples was conducted based on the analytical procedure of the National Renewable Energy Laboratory (NREL) using a two-step acid hydrolysis method. Sugar composition was analyzed by high performance anion exchange chromatography (HPEAC) on an ICS-3000 system (Dionex, CA) equipped with an electrochemical detector and CarboPac PA 20 analytical column. Acid-soluble lignin (ASL) and acid-insoluble lignin (AIL) were determined according to the NREL procedure (Sluiter *et al*. 2008a and b).

All assays were performed in duplicate. The chemical composition of the samples is summarized in Table 1.

Crystallinity measurement

FT-IR spectra of the lignin and pretreated samples were recorded using a Thermo Scientific Nicolet iN 10-MX FT-IR chemical imaging microscope (Thermo Scientific, USA) fitted with narrow-band liquid nitrogen cooled MCT detector. Spectra were recorded with 64 scans at a resolution of 4 cm^{-1} between 4000 and 800 cm^{-1}.

X-ray diffraction (XRD) analysis of the raw material, thermomechanical pulp, and the binderless boards were conducted using an XRD-600 X-ray Diffractometer (Shimadzu, Japan). Samples were pressed in a standard device to produce a pellet and scanned at 2 °/min from 5° to 35° with Ni-filtered Cu Kα radiation at 40 kV and 40 mA.

Solid-state cross-polarization/magic angle spinning (CP/MAS) ^{13}C NMR spectra of the raw material, thermomechanical pulp fiber and the binderless board were obtained on a Bruker AVIII 400 MHz spectrometer with a 4 mm zirconia (ZrO_2) rotor. The experiment was performed using a CP pulse program with 1 ms match time and a 2 s delay between transients. The number of scans was 5000 with a spinning rate 5 kHz. The crystallinity index was calculated according to Sun *et al.* (2013).

Gel permeation chromatography (GPC) analysis

The weight-average (M_w) and number-average (M_n) molecular weights of these lignin fractions were determined by GPC on a PL-gel 10 mm Mixed-B 7.5 mm i.d. column on an Agilent 1200 series high performance liquid chromatograph (HPLC) instrument. A differential refractive index detector (RID) was used. Lignin (2 mg) was dissolved in 1 mL of tetrahydrofuran (THF), and 20 μL lignin solution aliquots were injected with a THF flow rate of 1.0 mL/min. Monodisperse polystyrene was used as the standard for the molecular weight of lignin.

Quantitative ^{31}P NMR spectra

Quantitative ^{31}P NMR of the lignin fractions was carried out according to the published procedures (Argyropoulos 1994; Granata and Argyropoulos 1995; Akim *et al*. 2005). A solvent mixture composed of pyridine and deuterated chloroform (1.6:1, v/v) was prepared. An internal standard solution was prepared with cholesterol (400 mg) and chromium (III) acetylacetonate (40 mg) dissolved in 10 mL of the solvent mixture. Relaxation reagent was prepared with chromium (III) acetylacetonate (27.9 mg) dissolved in 5 mL of the solvent mixture. Approximately 25 mg of dry lignin was transferred into a sample vial, dissolved in 600 μL of solvent mixture with 100 μL of internal standard solution, and left at room temperature overnight with continuous stirring. Finally, 2-chloro-4,4,5,5,-tetramethyl-1,3,2,-dioxaphospholate (100 μL) was added, and the mixture was transferred into a NMR tube for analysis.

2D HSQC NMR spectra of the lignin

The 2D HSQC NMR spectra were also recorded on a Bruker AVIII 400 MHz spectrometer with a 5 mm BBI probe at 25 °C using DMSO-d_6 as the solvent. The Bruker standard pulse program in an echo/anti-echo acquisition mode (Bruker pulse program hsqcetgp) was used for the HSQC experiments.

RESULTS AND DISCUSSION

Chemical Analysis of the Binderless Boards

Table 1 shows the chemical compositions of the raw material, thermomechanical pulp, and the hot-pressed boards. As shown, the major sugars in all the samples were glucose and xylose. The Klason lignin content in the raw material and thermomechanical pulp were 28.51% and 22.26%, respectively. In the production of thermomechanical pulp fiber, lignin was softened, and a small amount of the lignin was degraded and lost into the solution, which was confirmed by the decreased content of AIL. Since the pretreatment by sodium silicate solution can increase the content of AIL of thermomechanical pulp, the amount of the AIL increased with increasing concentrations of sodium silicate. The results show that the content of AIL of the binderless board pretreated with 0.15% sodium silicate solution (BB15a) increased to 35.76%, which was higher than those of the raw material (28.51%) and thermomechanical pulp (22.26%). The increase of AIL was mainly due to solubilized sodium silicate, which can act as an adhesive that hardens like geopolymers to form a rigid, non-stoichiometric 3D structure, linking adsorbates into a composite structure (Vail 1952; Kouassi *et al*. 2011). Therefore, a sodium silicate glass coating seems to have surrounded the surface of the wood particle, which made the surface rough and stiff. Both the contents of ASL and AIL increased after hot pressing.

Table 1 also shows differences in carbohydrate content and sugar types between different BB samples. The carbohydrate contents of sugar were expected to play an important role in providing adhesion in BB (Shen 1986). Glucose and xylose were found to be the major sugars in these BB samples (Table 1). After hot pressing, the glucose content of BB increased slightly compared with the pretreated samples without hot pressing. The result indicates that the sugar content increased in the BB samples, probably due to degradation of hemicelluloses during hot pressing. The partial degradation of hemicellulose increases the compressibility of wood, reduces the tendency for stresses to be built-up in pressed composites, and lowers the springback of the compressed wood (Hsu *et al*. 1988; Pelaez-Samaniego *et al*. 2013).

Table 1. Chemical Composition of Raw Material, Thermomechanical Pulp, and Binderless Boards

Sample	Lignin content *** (%)		Carbohydrate content **** (%)						Total sugar (%)
	ASL	AIL	Rha	Ara	Gal	Glu	Xyl	GlcA	
RM *	3.18	28.51	0.70	0.40	1.33	48.26	21.35	1.36	73.40
TMP **	5.97	22.26	0.62	0.38	1.69	37.40	15.72	1.02	56.83
BB3b	5.21	32.14	0.80	0.37	1.38	42.32	22.03	1.12	68.02
BB3a	5.22	33.45	0.43	0.14	1.65	46.92	18.21	1.23	68.58
BB15b	5.12	29.04	0.53	0.25	1.49	39.28	16.74	0.93	58.69
BB15a	5.22	35.76	0.36	0.15	1.50	45.65	16.90	1.16	65.72

* RM, raw material. ** TMP, thermomechanical pulp.
*** ASL and AIL were calculated based on the Klason lignin of the corresponding samples.
**** Rha, rhamnose; Ara, arabinose; Gal, galactose; Glu, glucose; Man, mannose; Xyl, xylose; GlcA, glucuronic acid

Internal Bond (IB) Strength

The correlation between the chemical composition and IB strength of the BB is shown in Fig. 2.

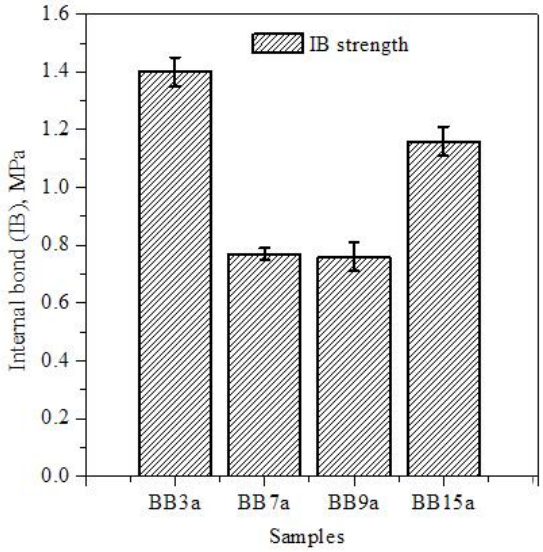

Fig. 2. The effect of chemical changes by sodium silicate solution pretreatment on internal bond strength of the binderless boards. BB3a, BB7a, BB9a, and BB15a represent the binderless boards, which were manufactured by 0.3%, 0.7%, 0.9%, and 1.5% sodium silicate solution pretreated thermomechanical pulp, respectively.

As can be seen in Fig. 2, the sodium silicate solution pretreatment was effective in increasing the IB strength of binderless boards. It should be noted that the BB treated with 0.3% and 1.5% sodium silicate solution resulted in a high IB strength of 1.40 and 1.16 MPa, respectively. These values were higher than the IB strength of samples made from the core of the trunk (0.71 MPa) (Hashim *et al.* 2011). The BB samples also satisfied the Chinese Standard GB/T 11718-2009. According to the Standard, board thickness ranged from 3.5 to 6 mm and requires 0.60 MPa for IB strength. The high IB strength of the pretreated samples can be explained by the high content of lignin in the BB samples, because lignin has been reported to play an important role in self-bonding boards (Okuda *et al*. 2006a). In addition, the high sugar content in the BB samples is a desirable property for BB production. This result is in agreement with the report by Murai *et al*. (2009), who concluded that high starch and sugar content in the core of the oil palm trunk appeared suitable for BB production.

Structural Features of the Raw Material and the Pressing Boards

Various pretreatment methods have the potential to change the cellulose crystal structures by disrupting inter- and intra-chain hydrogen bonding of cellulose fibrils (Mosier *et al*. 2005). The crystallinity index (CrI) of the thermomechanical pulp and the pretreated samples was measured by FT-IR, X-ray diffraction, and solid NMR spectroscopy, and the results are summarized in Table 2. The absorption ratios of $A1427\ cm^{-1}/A898\ cm^{-1}$ and $A1367\ cm^{-1}/A2900\ cm^{-1}$ in the FT-IR spectra are known as the lateral order index (LOI) and total crystallinity index (TCI), and determine the crystallinity of cellulose (Nelson and O'Connor 1964; Oh *et al*. 2005). The absorption band at 1423 cm^{-1} is assigned to the CH_2 scissoring motion that is strong in cellulose I and very weak in cellulose II and amorphous cellulose. However, the absorption band at 898 cm^{-1} assigned as C-O-C stretching at the β-(1→4) glycosidic linkage was weak and broad in cellulose I but strong and sharp in cellulose II and amorphous cellulose. Therefore, as shown in Table 2, LOI and TCI of BB increased slightly after hot pressing. In solid NMR analysis, CrI was calculated by dividing the area of the crystalline peak (integrating the peak from 87 to 91 ppm) by the total area assigned to the C4 peaks (integrating the region from 80 to 91 ppm) (Neman 2004). The CP-MAS method shows a high crystallinity (0.45) of BB15a, which is in agreement with the FT-IR analysis. In addition, a small change in cellulose crystallinity was observed in these pretreated samples and the corresponding binderless boards according to results of XRD.

Table 2. Structural Features of the Raw Material, Thermomechanical Pulp, and Binderless Boards

Sample	LOI	TCI	Crystallinity (CP-MAS)	Crystallinity (XRD)
RM	0.83	1.00	35%	45%
TMP	0.85	0.89	43%	46%
BB3b	0.91	0.94	42%	47%
BB3a	0.85	0.99	44%	48%
BB15b	0.78	0.95	43%	48%
BB15a	0.80	1.04	45%	49%

Yield of Lignin

As shown in Table 3, the yield of MWL (% Klason lignin) in raw material and thermomechanical pulp were 3.1 and 3.8%, respectively, which were low compared to previous reports (Ikeda *et al*. 2002; Hu *et al*. 2006). To investigate the difference between raw material and thermomechanical pulp, a further extraction was processed with alkaline ethanol, and the yield of lignin (33.2%) extracted from thermomechanical pulp was higher than that from raw material (8.7%). This result may be explained on the basis of the thermochemical pretreatment, which causes lignin to coalesce into lager molten bodies that migrate in and out of the cell wall and redeposit on the surface of plant cell walls. The re-localization of lignin can effectively enhance the lignin removal during the fractionation process (Donohoe *et al*. 2008). The dark brown color of the thermo-mechanical pulp also indicates that a high degree of hydrolysis or modification of the chemical components occurred during thermomechanical pulp process. In addition, one should note that the yield of EMAL from the 1.5% sodium silicate solution pretreated BB (BB15a) was 31.1%. However, the yields of EMAL from thermomechanical pulp and 1.5% sodium silicate solution pretreated thermomechanical pulp fiber before hot pressing (BB15b) were 55.8% and 54.9%, respectively. Hot pressing treatment was found have a large effect on the chemical composition of the BB, especially decreasing the yield of lignin. The pretreated thermomechanical pulp contained hemicelluloses such as glucuronoxylan and glucomannan. It may be hypothesized that a rigid network of lignin–carbohydrate complexes may have been formed under the effect of hot pressing, therefore making it difficult to extract lignin from the BB. This hypothesis is in accordance with a previous study by Widyorini *et al.* (2005), who found that different types of covalent linkages between lignin and hemicelluloses were formed during steam treatment of kenaf core for BB production.

Table 3. Yields of Klason Lignin

	RM	TMP	BB15b	BB15a
MWL	3.1%	3.8%	—	—
EMAL	—	55.8%	54.9%	31.1%

Molecular Weight Distributions

The values of the weight-average (M_w), number-average (M_n) molecular weights, and the polydispersity (M_w/M_n) of the MWL and EMAL are shown in Table 4. As can be seen, the MWL of thermomechanical pulp fiber showed relatively higher M_w (3385 g/mol) than any other lignin fractions, probably due to the lignin polycondensation in thermomechanical pulp process. The EMAL extracted from BB15b had a higher value of M_w (2210 g/mol) than those from thermomechanical pulp and BB15a (M_w, 1630 g/mol), suggesting that the sodium silicate pretreatment can coalesce lignin to a large molecular weight, which was effective in BB production. However, after hot pressing treatment, the M_w of EMAL decreased to 1630 g/mol. This shows that the lignin was degraded to a certain degree by hot pressing, and the lignin with small molecular weight could be easily extracted from the hot-pressing boards. The degradation of lignin can increase the compressibility of boards and reduce the internal stress induced in each particle, which can enhance the board performance (Widyorini *et al*. 2005). In addition, high polydispersity (4.15 to 3.49) of EMAL was observed (Table 4), suggesting that some

components of lignin were modified by hot pressing. The high polydispersity indicated an inhomogeneous molecular structure of lignin, especially for the sodium silicate solution pretreated samples.

Table 4. Weight-average (M_w, g/mol) and Number-average (M_n, g/mol) Molecular Weights and Polydispersity (M_w/M_n) of the Lignin Fractions

	Lignin fraction				
	RM-MWL	TMP-MWL	TMP-EMAL	BB15b-EMAL	BB15a-EMAL
M_w	2320	3385	1580	2210	1630
M_n	670	2250	450	530	430
M_w/M_n	3.47	1.50	3.49	4.15	3.80

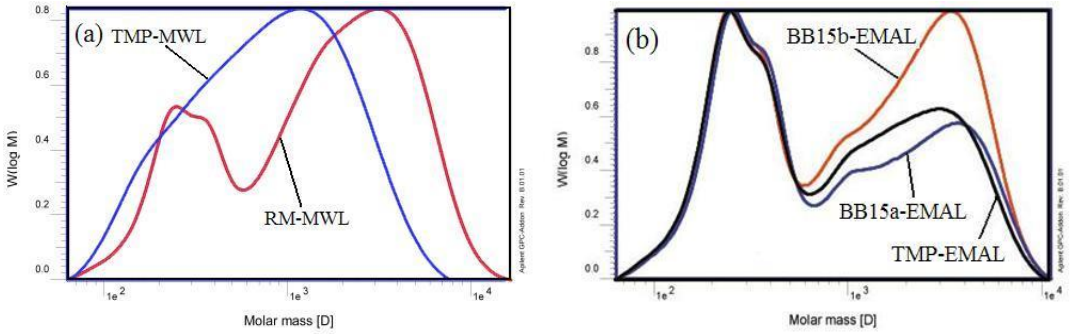

Fig. 3. Molecular weight distributions of the lignin fractions MWL (a) and EMAL (b)

The molecular weight distribution curves of MWL isolated from thermo-mechanical pulp showed a wide and high peak, indicating a large and uniform size of lignin molecular (Fig. 3a). Comparatively, other lignin fractions exhibited two peaks, as can be observed from the GPC curves (Fig. 3b). This observation clearly indicated an inhomogeneous distribution of lignin molecules, which was in line with the poly-dispersity values.

FT-IR Spectra Analysis

Figure 4 shows the FT-IR spectra of the lignin fractions. A number of bands were used to monitor the chemical changes that occurred in the pretreatment process. The MWL of raw material exhibited a wide and strong absorption band at 1721 cm^{-1}, which is assigned to C=O stretching of unconjugated ketone, carbonyl, and ester groups (Fig. 4a). This signal was decreased in the MWL spectra of thermomechanical pulp. The MWL showed strong peaks at 1122 cm^{-1} (assigned to C-C, C-O, and C=O stretching and aromatic C-H deformation in S unit) as compared to the MWL of raw material. This demonstrates that the content of S-type lignin increased in the thermomechanical pulp. The peak around 1653 cm^{-1} in EMAL of the BB15a and BB15b samples indicated the presence of conjugated ketone and carbonyl compounds in low molecular weight compounds (Okuda *et al.* 2006b) (Fig. 4b). These compounds were considered to be associated with self-bonding, and may contribute to the improvement of the board properties. The bands at 1594, 1504, and 1422 cm^{-1} are assigned to the characteristic stretching of structural benzene ring in lignin. The C-H deformation and aromatic ring vibrations at 1458 and 1461 cm^{-1} are present in these spectra (Faix 1991). Syringyl (S)

and condensed guaiacyl (G) absorptions were observed at 1327 cm^{-1}, whereas the small shoulder peak at 1271 cm^{-1} was due to G unit ring breathing with C=O stretching, indicating that small amounts of G unit lignin were present in MWL and EMAL. In addition, the EMAL of binderless board (BB15a) and sodium silicate solution pretreated sample (BB15b) showed a relatively strong absorption band at 1124 cm^{-1} compared to thermomechanical pulp, suggesting a high content of S unit lignin existed in the pretreated thermomechanical pulp and the binderless board. Therefore, it can be concluded that sodium silicate solution treatment and hot pressing can increase the content of S unit lignin. In addition, the absorption bands at 1031 to 1034 and 830 to 834 cm^{-1} are considered to be the aromatic C-H in-plane and out-of-plane deformation of aromatic rings, respectively.

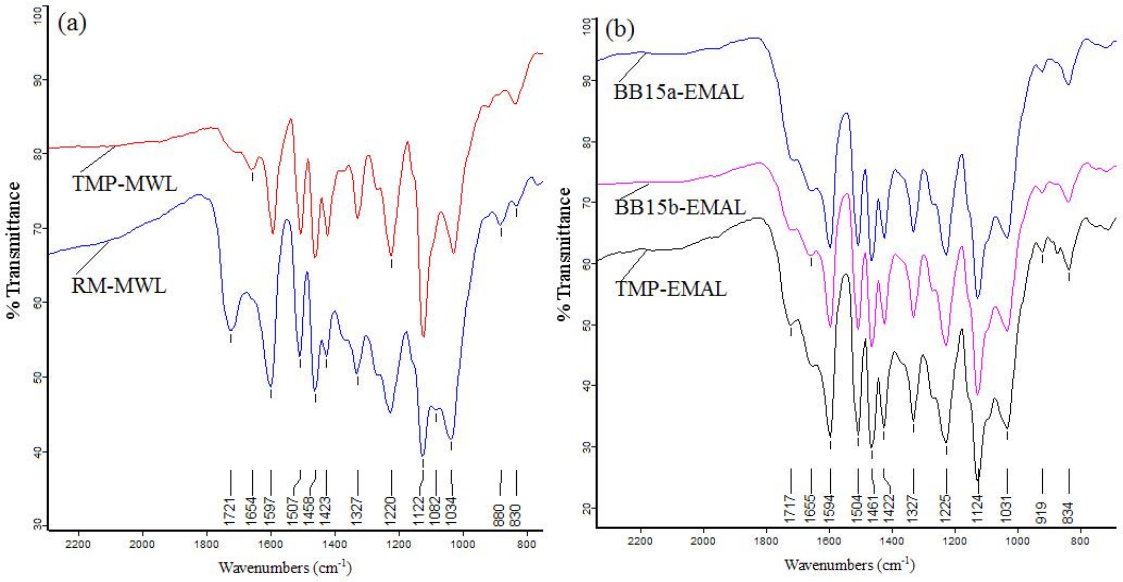

Fig. 4. FT-IR spectra of the lignin fractions MWL (a) and EMAL (b) isolated from raw material, thermomechanical pulp, and binderless boards

Quantitative ^{31}P NMR

Phosphitylation followed by quantitative ^{31}P NMR analysis was conducted to determine various chemical functionalities of lignin. The methodology is based on the phosphitylation reaction of aliphatic hydroxyls, condensed and non-condensed phenolic hydroxyls, and carboxylic acids groups in lignin, which in turn improves the solubility of the samples and makes the various OH groups detectable. Details of signal acquisition, assignment, and integration can be found elsewhere (Granata and Argyropoulos 1995; Akim *et al*. 2005). Table 5 lists the quantitative data on the distribution of the various OH groups of these lignin fractions.

As can be seen in Table 5, the content of phenolic OH groups of MWL from thermomechanical pulp decreased relative to MWL from raw material, with the exception of the non-condensed S (NS) unit. A small amount of total phenolic OH groups (3.83 mmol/g) of MWL from thermomechanical pulp was also observed. The significant decrease in condensed G (CG) and non-condensed G (NG) units indicated that G-type lignin was more easily degraded in the thermomechanical pulp process than S-type lignin. The aliphatic OH group of EMAL from thermomechanical pulp was 3.82 mmol/g, which was higher than that in MWL from thermomechanical pulp. The EMAL from

thermomechanical pulp showed high total phenolic OH group (4.45 mmol/g). However, the decreased OH group (2.78 mmol/g) observed in the pretreatment sample (BB15b) suggests that the condensation reaction between lignin and sodium silicate did occur. When hot pressing was performed, the phenolic OH group of the BB increased to 3.97 mmol/g. The increased OH group content was due to the degradation of lignin. In addition, the cleavage of the lignin-carbohydrate linkages may be another reason for the high content of the aliphatic OH group, since a high content of carbohydrates (65.72%) was observed in BB15a. Most carbohydrates are connected to the α-carbon of the lignin phenyl propane unit, and the cleavage of this lignin-carbohydrate bond during hot pressing liberates a new α-hydroxyl group (Jääskeläinen *et al.* 2003). These functional groups may have contributed to some improvement of the bonding properties. Moreover, the content of COOH groups was stable in the EMAL fractions, probably because the oxidation reaction of lignin was inconspicuous during the hot pressing process.

Table 5. Content of the Various Hydroxyl Groups (mmol/g) of Lignin Quantified by ^{31}P NMR

		Phenolic OH *					Total phenolic	Carboxylic acid
Sample	Aliphatic	CS	NS	CG	NG	NH		
RM-MWL	3.98	0.09	0.24	0.24	0.69	0.23	5.47	0.15
TMP-MWL	3.03	0.06	0.33	0.05	0.34	0.02	3.83	0.17
TMP-EMAL	3.82	0.04	0.26	0.06	0.25	0.02	4.45	0.03
BB15b-EMAL	2.56	0.01	0.13	0.01	0.07	ND	2.78	0.02
BB15a-EMAL	3.47	0.03	0.25	0.04	0.14	0.04	3.97	0.03
* CS: Condensed S, NS: Non-condensed S, CG: Condensed G, NG: Non-condensed G, NH: Non-condensed H, ND: Not determined								

2D HSQC NMR Spectra

In order to obtain more detailed chemical information of the lignin fractions, 2D NMR is required. Figure 5 shows the side-chain and aromatic regions of the HSQC spectra for the isolated lignin.

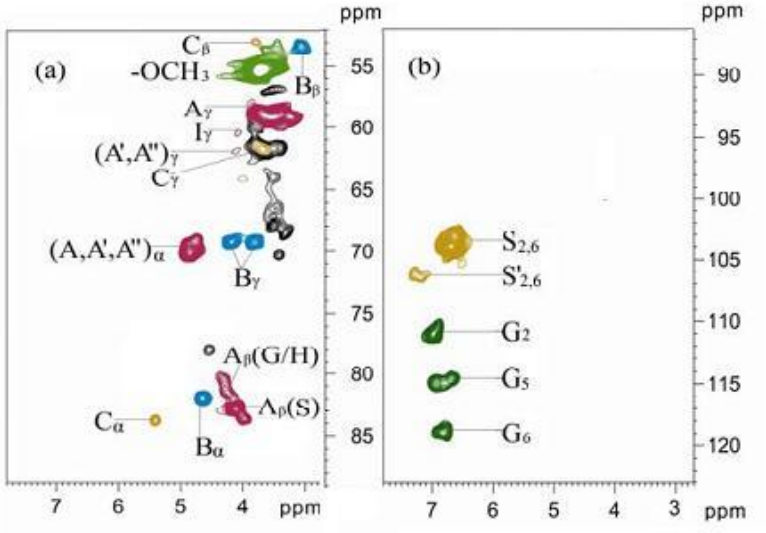

Fig. 5. 2D HSQC NMR spectra of lignin fractions: side-chain (a) and aromatic (b) regions

The aliphatic (nonoxygenated) region showed signals with no structural information and therefore is not discussed here. The main lignin cross-signals assigned in the HSQC spectra are listed in Table 6, and the main substructures are depicted in Fig. 6.

Table 6. Assignment of Main Lignin ^{13}C-^{1}H Cross-signals

Label	δ_H/δ_C (ppm)	Assignment
C_β	53.0/3.45	C_β-H_β in β-5′ (phenylcoumaran) substructures (**C**)
B_β	53.4/3.05	C_β-H_β in β-β′ (resinol) substructures (**B**)
-OMe	55.6/3.73	C-H in methoxyls
$(A, A', A'')_\gamma$	59.4/3.38, 3.67	C_γ-H_γ in γ-acetylated β-O-4′ substructures (**A/A′/A"**)
I_γ	61.3/4.12	C_γ-H_γ in p-hydroxycinnamyl alcohol end-groups (**I**)
C_γ	62.5/3.67	C_γ-H_γ in β-5′ (phenylcoumaran) substructures (**C**)
B_γ	70.9/3.82, 4.17	C_γ-H_γ in β-β′ (resinol) substructures (**B**)
$(A, A', A'')_\alpha$	71.6/4.84	C_α-H_α in β-O-4′ substructures linked to a S unit (**A/A′/A"**)
$A_{\beta(G/H)}$	83.5/4.29	C_β-H_β in β-O-4′ substructures linked to a G or H unit (**A**)
B_α	84.8/4.64	C_α-H_α in β-β′ (resinol) substructures (**B**)
$A_{\beta(S)}$	85.6/4.11	C_β-H_β in β-O-4′ substructures linked to a S unit (**A**)
C_α	86.6/5.47	C_α-H_α in β-5′ (phenylcoumaran) substructures (**C**)
$S_{2,6}$	104.0/6.69	$C_{2,6}$-$H_{2,6}$ in syringyl units (**S**)
$S'_{2,6}$	106.1/7.29	$C_{2,6}$-$H_{2,6}$ in C_α-oxidized (C_α=O) phenolic syringyl units (**S′**)
G_2	111.0/6.97	C_2-H_2 in guaiacyl units (**G**)
G_5	114.8/6.93 and 114.4/6.71	C_5-H_5 in guaiacyl units (**G**)
G_6	118.9/6.81	C_6-H_6in guaiacyl units (**G**)

In the side-chain (δ_C/δ_H 50-90/2.5-7.5 ppm) regions, the cross-signals of β-O-4' substructures were the most prominent. The C_α-H_α correlation in β-O-4' aryl ether linkages were observed at δ_C/δ_H 71.6/4.84 (structures **A**, **A'**, and **A''**). The C_β-H_β correlations in β-O-4' substructures linked to S-type and G/H type lignin can be clearly distinguished at 85.6/4.11 and 83.5/4.29, respectively. The HSQC spectra demonstrated that the MWL of raw material was acetylated, and acylation took place only at the γ-position of the side-chain. However, the signals of C_γ-H_γ of β-O-4' aryl ether linkages with acetylated –OH at γ-carbon (**A'**) and with *p*-hydroxybenzoated –OH at γ-carbon (**A''**) could not be detected in the EMAL fractions of BB15b and BB15a, indicating the cleavage of ester groups of lignin during pulping and hot pressing processes.

Signals for other lignin substructures were also observed in the HSQC spectra, corresponding to minor structures. The signals for resinol (β-β'/α-O-γ'/γ-O-α') substructures (**B**) were observed in the HSQC spectra of MWL and EMAL, with their C_α-H_α, C_β-H_β, and the double C_γ-H_γ correlations at δ_C/δ_H 84.8/4.64, 53.4/3.05 and 70.9/3.82, and 4.17, respectively. Phenylcoumaran (β-5'/α-O-4') substructures (**C**) were observed in the HSQC spectra for their C_α-H_α, C_β-H_β correlations at δ_C/δ_H 86.6/5.47 and 53.0/3.45, respectively, and C_γ-H_γ correlation overlapping with xylan C_5-H_5 cross-signals around δ_C/δ_H 62.5/3.67. It should be noted that the signals for spirodienone structure were not obvious in the HSQC spectra due to its low abundance in raw material and thermomechanical pulp. In addition, cinnamyl alcohol end-groups (**I**) was observed not only in the HSQC spectra of MWL of starting material, but also in the spectra of EMAL

of the hot-pressing boards. Finally, it was shown that EMAL contained less content of carbohydrate as compared to MWL.

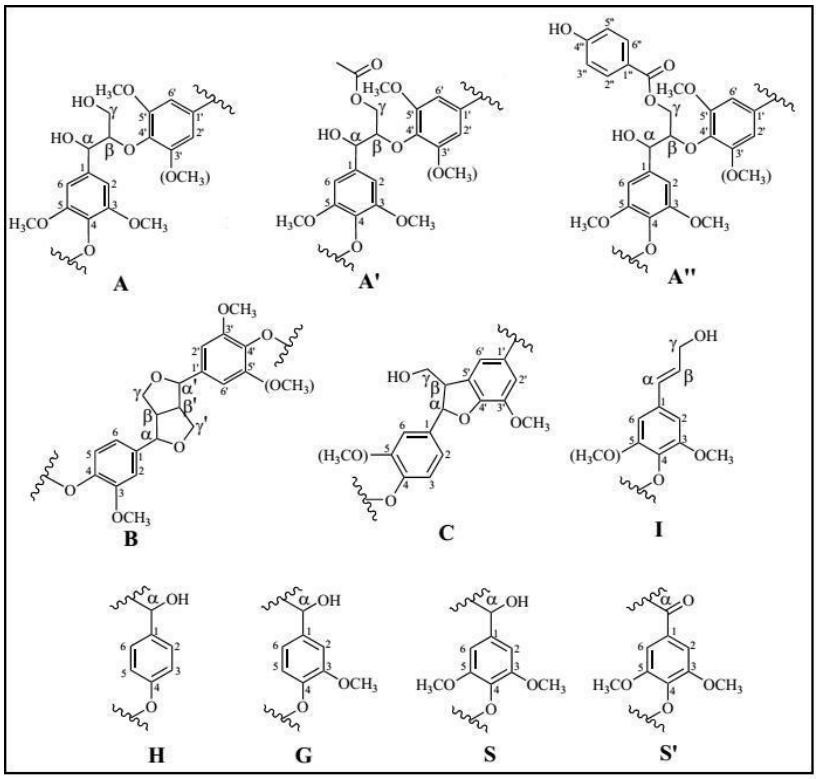

Fig. 6. Main classical and acetylated substructures, involving different side-chain linkages, and aromatic units identified by 2D NMR of eucalyptus lignin: (**A**) β-O-4' aryl ether linkages with a free –OH at the γ-carbon; (**A'**) β-O-4' aryl ether linkages with acetylated –OH at the γ-carbon; (**A''**) β-O-4' aryl ether linkages with *p*-hydroxybenzoated –OH at γ-carbon; (**B**) resinol substructures formed by β-β', α-O-γ', and γ-O-α' linkages; (**C**) phenylcoumaran substructures formed by β-5' and α-O-4' linkages; (**I**) *p*-hydroxycinnamyl alcohol end groups; (**H**) *p*-hydroxyphenyl units; (**G**) guaiacyl units; (**S**) syringyl units; (**S'**) oxidized syringyl units with a C_α ketone

In the aromatic regions, the *p*-hydroxyphenyl (**H**) unit could not be observed in EMAL, but it could be observed in MWL. Signals corresponding to C_α-oxidized (C=O) **S** units (**S'**$_{2,6}$, δ_C/δ_H 106.1/7.29) were present in all of the lignin fractions, indicating that this moiety might exist in the lignin of the starting material, and their provenance from the milling and hot pressing processes cannot be completely ruled out. The **S** unit showed a prominent signal for the $C_{2,6}$-$H_{2,6}$ correlation at δ_C/δ_H 104.0/6.69, while the **G** unit showed different correlations for C_2-H_2 (δ_C/δ_H 111.0/6.97), C_5-H_5 (δ_C/δ_H 114.8/6.93 and 114.4/6.71), and C_6-H_6 (δ_C/δ_H 118.9/6.81). The double C_5-H_5 correlations was probably due to different substituents at the C_4 position (e.g., phenolic or etherified in different substructures) (Rencoret *et al*. 2009).

The different structural features among the lignin specimens were semi-quantitatively investigated. The percentage of substructures **A**-**I** and **S** to **G** ratios was calculated and summarized in Table 7. The main substructures present in the raw material, the thermomechanical pulp, and the hot-pressing boards were β-O-4' aryl ether (**A**, **A'**, **A''**) linkages. The results showed that the acidic dioxane extraction procedure could

preserve more content of β-O-4' linkages. In addition, the content of β-O-4' linkages of the pretreated thermomechanical pulp (BB15b) was 62.6%, which was somewhat higher than that of thermomechanical pulp (60.1%). The effect of sodium silicate solution pretreatment on lignin can be deduced. Moreover, the hot-pressing board (BB15a) showed a remarkable increase of β-O-4' linkages (69.2%), suggesting that hot pressing was effective to enhance the production of β-O-4' linkages. Thus, it can be concluded that recondensation and depolymerization of lignin were two competing reactions during hot pressing. The degradation of β-O-4' linkages can result in a decreased M_w of lignin as observed by GPC analysis, while the condensation reaction usually leads to the increase of β-O-4' linkages. In addition, the secondary major β-β' resinol substructure (**B**) increased by 1% after hot pressing, while the β-5' phenylcoumaran substructure (**C**) slightly decreased.

Table 7. Structural Characteristics from Integration of ^{1}H-^{13}C Correlation Signals in the HSQC Spectra of the Lignin Fractions

Characteristic	RM-MWL	TMP-MWL	TMP-EMAL	BB15b-EMAL	BB15a-EMAL
β-O-4' aryl ether (**A**, **A'**, **A"**)	50.3%	50.3%	60.1%	62.6%	69.2%
Resinol (**B**)	8.3%	12.2%	7.0%	8.0%	8.0%
Phenylcoumaran (**C**)	3.3%	3.1%	1.5%	1.5%	1.3%
Cinnamyl alcohol end-groups (**I**)	2.0%	0.2%	0.5%	1.1%	0.7%
S to G (HSQC)	1.33	2.44	2.85	3.66	4.06

The syringyl-guaiacyl (**S**/**G**) ratios are shown in Table 7. The **S**/**G** ratio from this experiment was calculated to be 4.06 for the hot-pressing board (BB15a). This value is higher than what is observed in ordinary lignocellulosic materials, such as eucalypt wood (**S**/**G**, 2.8) and kenaf core (**S**/**G**, 1.5-2.0) (Ohtani *et al*. 2001; Rencoret *et al*. 2009). The **S**/**G** ratios increased compared to the pretreated sample (BB15b) and thermomechanical pulp. It was found that substructures containing **S** unit are preferentially condensed by hot pressing over those containing **G** unit, and **G** unit are easier to decompose than **S** unit. This result was in accordance with the FT-IR analysis, which showed a high amount of **S** unit lignin present in the hot-pressing boards. More importantly, the **G** unit decomposing to vanillin during hot pressing may play a role as a lignin plasticizer (Bouajila *et al*. 2005). The data demonstrated that chemical modification of lignin from binderless boards is significant by hot pressing treatment.

CONCLUSIONS

1. Sodium silicate solution pretreatment was found to be an effective method for the improvement of the binderless board properties.
2. The acid insoluble lignin of the pretreated samples increased with increasing concentrations of sodium silicate solution. The sugar content and the crystallinity of the binderless boards increased by the hot-pressing process.

3. The EMAL extracted from pretreated sample showed a high M_w (2210 g/mol), suggesting that the sodium silicate pretreatment could coalesce lignin to a large molecular weight. However, the M_w of lignin decreased to 1630 g/mol after hot pressing.
4. Quantitative ^{31}P NMR analysis showed that the total phenolic OH groups in EMAL from binderless boards increased relative to the pretreated sample.
5. HSQC results indicated an increase of β-O-4' linkages (69.2%) in the EMAL of binderless boards. In addition, lignin containing **S** unit are preferentially condensed by hot pressing over those containing **G** unit, and **G** unit are easier to decompose than **S** unit.

ACKNOWLEDGMENTS

The authors are extremely grateful for the financial support from the National Science and Technology Program of the 12th Five-Year Plan Period (2012BAD32B06) and National Science Foundation of China (30800868).

REFERENCES CITED

Akim, L. G., Argyropoulos, D. S., Jouanin, L., Leplé, J. C., Pilate, G., Pollet, B., and Lapierre, C. (2005). "Quantitative ^{31}P NMR spectroscopy of lignins from transgenic poplars," *Holzforschung* 55(4), 386-390.

Argyropoulos, D. S. (1994). "Quantitative phosphorus-31 NMR analysis of lignins, a new tool for the lignin chemist," *J. Wood Chem. Technol.* 14(1), 45-63.

Bhagat, S., Kim, Y. H., Ahn, Y. S., and Yeo, J. G. (2007). "Rapid synthesis of water-glass based aerogels by in situ surface modification of the hydrogels," *Appl. Surf. Sci.* 253 (6), 3231-3236.

Björkman, A. (1956). "Studies on finely divided wood I. Extraction of lignin with neutral solvents," *Svensk Papperstidning* 59(13), 477-485.

Bouajila, J., Limare, A., Joly, C., and Dole, P. (2005). "Lignin plasticization to improve binderless fiberboard mechanical properties," *Polym. Eng. Sci.* 45(6), 809-816.

Donohoe, B. S., Decker, S. R., Tucker, M. P., Himmel, M. E., and Vinzant, T. B. (2008). "Visualizing lignin coalescence and migration through maize cell walls following thermochemical pretreatment," *Biotechol. Bioeng.* 101(5), 913-925.

Ellis, S., and Paszner, L. (1994). "Activated self-bonding of wood and agricultural residues," *Holzforschung* 48(s1), 81-90.

Enoki, A., Tanaka, H., and Fuse, G. (1988). "Degradation of lignin-related compounds, pure cellulose and wood components by white-rot and brown-rot fungi," *Holzforschung* 42(2), 85-93.

Faix, O. (1991). "Classification of lignins from different botanical origins by FT-IR spectroscopy," *Holzforschung* 45(s1), 21-27.

Granata, A., and Argyropoulos, D. S. (1995). "2-Chloro-4,4,5,5-tetramethyl-1,3,2-dioxaphospholane, a reagent for the accurate determination of the uncondensed and condensed phenolic moieties in lignins," *J. Agric. Food Chem.* 43(6), 1538-1544.

Hashim, R., Nadhari, W. N. A., Sulaiman, O., Kawamura, F., Hiziroglu, S., Sato, M., Sugimoto, T., Seng, T. G., and Tanaka, R. (2011). "Characterization of raw materials and manufactured binderless particleboard from oil palm biomass," *Mater. Des.* 32(1), 246-254.

Hsu, W. E., Schwald, W., Schwald, J., and Shields, J. A. (1988). "Chemical and physical changes required for producing dimensionally stable wood-based composites, Part 1: Steam pretreatment," *Wood Sci. Technol.* 22(3), 281-289.

Hu, Z. J., Yeh, T. F., Chang, H. M., Matsumoto, Y., and Kadla, J. F. (2006). "Elucidation of the structure of cellulolytic enzyme lignin," *Holzforschung* 60(4), 389-397.

Ikeda, T., Holtman, K., Kadla, J., Chang, H., and Jameel, H. (2002). "Studies on the effect of ball milling on lignin structure using a modified DFRC method," *J. Agri. Food Chem.* 50(1), 129-135.

Jääskeläinen, A. S., Sun, Y., Argyropoulos, D. S., Tamminen, T., and Hortling, B. (2003). "The effect of isolation method on the chemical structure of residual lignin," *Wood Sci. Technol.* 37(2), 91-102.

Kouassi, S. S., Tognonvi, M. T., Soro, J., and Rossignol, S. (2011). "Consolidation mechanism of materials from sodium silicate solution and silica-based aggregates," *J. Non-Cryst. Solids* 357(15), 3013-3021.

Laemsak, N., and Okuma, M. (2000). "Development of boards made from oil palm frond II: properties of binderless boards from steam-exploded fibers of oil palm frond," *J. Wood Sci.* 46(4), 322-326.

Mobarak, F., Fahmy, Y., and Augustin, H. (1982). "Binderless lignocelluloses composite from bagasse and mechanism of self-bonding," *Holzforschung* 36(3), 131-135.

Mosier, N., Wyman. C., Dale. B., Elander, R., Lee, Y. Y., Holtzapple, M., and Ladisch, M. (2005). "Features of promising technologies for pretreatment of lignocellulosic biomass," *Bioresour. Technol.* 96(6), 673-686.

Murai, K., Uchida, R., Okubo, A., and Kondo, R. (2009). "Characterization of the oil palm trunk as a material for bio-ethanol production," *Mokuzai Gakkaishi* 55(6), 346-355.

Nelson, M. L., and O'Connor, R. T. (1964). "Relation of certain infrared bands to cellulose crystallinity and crystal lattice type. Part II. A new infrared ratio for estimation of crystallinity in cellulose I and II," *J. Appl. Polym. Sci.* 8(3), 1325-1341.

Neman, R. H. (2004). "Homogeneity in cellulose crystallinity between samples of *Pinus radiata* wood," *Holzforschung* 58(1), 91-96.

Oh, S. Y., Yoo, D. I., Younsook, S., Kim, H. C., Kirn, H. Y., Chung, Y. S., Park, W. H., and Youk, J. H. (2005). "Crystalline structure analysis of cellulose treated with sodium hydroxide and carbon dioxide by means of X-ray diffraction and FTIR spectroscopy," *Carbohydr. Res.* 340(15), 2376-2391.

Ohtani, Y., Mazumder, B. B., and Saseshima, K. (2001). "Influence of chemical composition of kenaf bast and core in the alkaline response," *J. Wood Sci.* 47(1), 30-35.

Okamoto, H., Sano, S., Kawai, S., Okamoto, T., and Sasaki, H. (1994). "Production of dimensionally stable medium density fiberboard by use of high-pressure steam pressing (in Japanese)," *Mokuzai Gakkaishi* 40(4), 380-389.

Okuda, N., Hori, K., and Sato, M. (2006a). "Chemical changes of kenaf core binderless boards during hot pressing (II): Effects on the binderless board properties," *J. Wood Sci.* 52(3), 249-254.

Okuda, N., Hori, K., and Sato, M. (2006b). "Chemical changes of kenaf core binderless boards during hot pressing (I): Influence of the pressing temperature condition," *J. Wood Sci.* 52(3), 244-248.

Pelaez-Samaniego, M. R., Yadama, V., Lowell, E., and Espinoza-Herrera, R. E. (2013). "A review of wood thermal pretreatments to improve wood composite properties," *Wood Sci. Technol.* 47(6), 1285-1319.

Rencoret, J., Marques, G., Gutiérrez, A., Nieto, L., Ignacio Santos, J., Jiménez-Barbero, J., Martínez, Á. T., and del Río, J. C. (2009). "HSQC-NMR analysis of lignin in woody (*Eucalyptus globulus* and *Picea abies*) and non-woody (*Agave sisalana*) ball-milled plant materials at the gel state," 10th EWLP, Stockholm, Sweden, August 25-28," *Holzforschung* 63(6), 691-698.

Rokiah, H., Siti Hazneza, A. H., Othman, S., Norli, I., Hakimi, I. M., Hasnah, M. J., and Salmiah, U. (2009). "Extractable formaldehyde from waste medium density fibreboard," *J. Trop. Forest Sci.* 21(1), 25-33.

Satoh, A. (1999). "Water glass bonding," *Sensors Actuators A: Phys.* 72(2), 160-168.

Shen, K. C. (1986). "Process for manufacturing composite products from lignocellulosic materials," United States Patent 4627951.

Sluiter, A., Hames, B., Ruiz, R., Scarlata, C., Sluiter, J., and Templeton, D. (2008a). "Determination of structural carbohydrates and lignin in biomass," LAP-002 NREL Analytical Procedure, National Renewable Energy Laboratory.

Sluiter, A., Hames, B., Ruiz, R, Scarlata, C., Sluiter, J., and Templeton, D. (2008b). "Determination of ash in biomass," LAP-005 NREL Analytical Procedure, National Renewable Energy Laboratory.

Sun, Y. C., Xu, J. K., Xu, F., and Sun, R. C. (2013). "Structural comparison and enhanced enzymatic hydrolysis of eucalyptus cellulose via pretreatment with different ionic liquids and catalysts," *Process Biochem.* 48(5-6), 844-852.

Suzuki, S., Shintani, H., Park, S. Y., Saito, K., Laemsak., N., Okuma, M., and Iiyama, K. (1998). "Preparation of binderless boards from steam exploded pulps of oil palm (*Elaeis guineensis* Jacq.) fronds and structural characteristics of lignin and wall polysaccharides in steam exploded pulps to be discussed for self-bonding," *Holzforschung* 52(4), 417-426.

Vail, J. G. (1952). *Soluble Silicates: Their Properties and Uses*, Rheinhold, New York.

Widyorini, R., Xu, J. Y., Watanabe, T., and Kawai, S. (2005). "Chemical changes in steam-pressed kenaf core binderless particleboard," *J. Wood Sci.* 51(1), 26-32.

Wu, S., and Argyropoulos, D. (2003). "An improved method for isolating lignin in high yield and purity," *J. Pulp Pap. Sci.* 29(7), 235-240.

Xu, J. Y., Han, G. P., Wong, E. D., and Kawai, S. (2003). "Development of binderless particleboard from kenaf core using steam-injection pressing," *J. Wood Sci.* 49(4), 327-332.

Yachi, A., Takahashi, R., Sato, S., Sodesawa, T., Oguma, K., Matsutani, K., and Mikami, N. (2005). "Silica gel with continuous macropores prepared from water glass in the presence of poly (acrylic acid)," *J. Non-Cryst. Solids* 351(4), 331-339.

Article submitted: November 27, 2013; Peer review completed: December 17, 2013; Revised version received and accepted: December 20, 2013; Published: January 3, 2014.